Doubly oriented β-form films of poly(vinylidene fluoride)

Toshiya Mizuno, Ken'ichi Nakamura, Naohiro Murayama and Kensuke Okuda

Kureha Chemical Industries Co. Ltd., Nishiki Research Laboratories, 16, Ochiai, Nishiki-machi, Iwaki-city, Fukushima, Japan 974

(Received 14 November 1983; revised 25 April 1984)

PVDF sheets, rapidly quenched, were (1) two-step transversely stretched at various temperatures and (2) stretched at various temperatures, rolled at room temperature and then annealed. The orientation patterns of the β-form crystal (which contains the polar b-axis) in these films were analysed on the basis of X-ray diffraction photographs taken with flat and cylindrical cameras. In the case of (1), when both of the two-step transversely stretching temperatures were below 100°C, a doubly oriented film with the polar b-axis oriented parallel to the film surface was obtained. In the case of (2), when the stretching temperature was below 100°C, the sheets then rolled without annealing, another doubly oriented film with the polar b-axis preferentially oriented at 30° to the film surface was obtained. On the other hand, when these films were annealed above 100°C, or the stretching temperatures were above 100°C, orientation patterns in which the polar b-axis was partially rotated through 60° were obtained. The orientation mechanisms of these films are discussed using the measurements of the lattice spacings of the β-form crystal.

(Keywords: poly(vinylidene fluoride); double orientation; X-ray cylindrical camera; pseudo-hexagonal crystal structure; stretching; rolling; annealing)

INTRODUCTION

Poly(vinylidene fluoride) (PVDF) is currently one of the most interesting polymers because it shows the highest piezoelectric effect in its polarized state[1]. PVDF shows polymorphism; it has four crystal structures; α, β, γ and polar α forms[2-7]. However, it is the β-form structure which shows the strongest piezoelectric effect.

In order to obtain a detailed understanding of this piezoelectric effect, we need to investigate the relationship between the orientation of dipoles and the piezoelectricity. One of the best ways of doing so is probably to obtain doubly oriented films[9] because such films will eliminate the ambiguity of the orientation. The doubly oriented film is also a partial model of the single crystal, and thus it is also very useful for a structure analysis of the crystalline polymer. At the same time, we might obtain a new film having particular properties which cannot be expressed for randomly oriented films.

A doubly oriented film of PVDF, however, has not yet been produced with an exception of T. T. Wang's 'single crystal orientation film' which was prepared by a combination of stretching, rolling and annealing processes[10]. It is known that there is no preferred orientation of the b-axis, which is the polar axis of the β-form crystal of PVDF, in uniaxially oriented films[11].

We have succeeded in obtaining a doubly oriented film in which the b-axis is parallel to the film surface. We tried to obtain a film which has the b-axis perpendicular to the film surface by following Wang's procedures, however we could not obtain a perfect sample. The film we produced has an orientation of the b-axis at 60° to the direction normal to the film surface.

In this paper, we will show the results of our structural analysis of these films using X-ray diffraction techniques. Measurements of the lattice spacings of these films are used to explain how the double orientations could take place during the processing procedures.

EXPERIMENTAL

The PVDF resin manufactured by Kureha Chemical Industry Co. Ltd. was used. $\eta_{inh.}$ is 1.35 (dl/g) measured at 30°C in 0.4 wt% dimethylformamide solution. The resin was moulded with a press at 250°C and then quenched in ice water as rapidly as possible. The sheets (0.5 mm thick × 5 cm long × 8 cm wide) were stretched at a temperature (T_1) using a tensile testing machine and a thermostat, to 3.5 times theor original length and then cooled immediately. These uniaxially stretched films (0.15 mm × 3 cm × 8 cm) were then stretched at a temperature (T_2) about 6 times, in the direction perpendicular to the first stretching direction, and cooled to room temperature immediately. The final films were about 0.04 mm × 18 cm × 3 cm in size. Since the edge regions of these films were not stretched well, only the inner sections were used. The procedure will be referred to as a 'two-step transversely stretching (T_1–T_2)'. A doubly oriented film was obtained by this procedure, the c-axis and the b-axis were oriented parallel to the stretching direction and the film surface, respectively.

The sheets (1.5 mm × 2 cm × 5 cm) were stretched in a similar manner to before at a temperature (T_3). The sheets were then rolled at room temperature (T_R) with a pair of steel rollers along the first stretching direction several times until half the original thickness was reached. The procedure is nearly the same one as adopted by Wang[10]

0032-3861/85/060853-06$03.00

and will be referred to as a 'two-step stretching and rolling ($T_3 - T_R$)'. By this procedure, doubly oriented films were obtained in which the *b*-axis and the *c*-axis are oriented at an angle of 60° to the direction normal to the film surface and parallel to the stretching and rolling directions, respectively.

The wide-angle X-ray scattering photographs were taken with flat and cylindrical cameras using a Ni-filtered CuKα radiation at 15 mA–35 kV.

The doubly oriented films obtained were too thin to give satisfactory X-ray diffraction patterns and therefore a number of 1 mm × 1 mm sheets had to be stacked together. These samples provide three mutually perpendicular axes. These are generally known as 'through', 'edge' and 'end' views. The sample arrangement for the tri-direction X-ray patterns is indicated in *Figure 1*.

The polymer chain axis (*c*-axis) of the *β*-crystal in these films is oriented along the second stretching or the rolling direction and the doubly oriented films are expressed as ϕ_b-oriented films and the double orientation as ϕ_b-orientation, where ϕ_b is the angle of the *b*-axis of the crystal to the direction normal to the film surface.

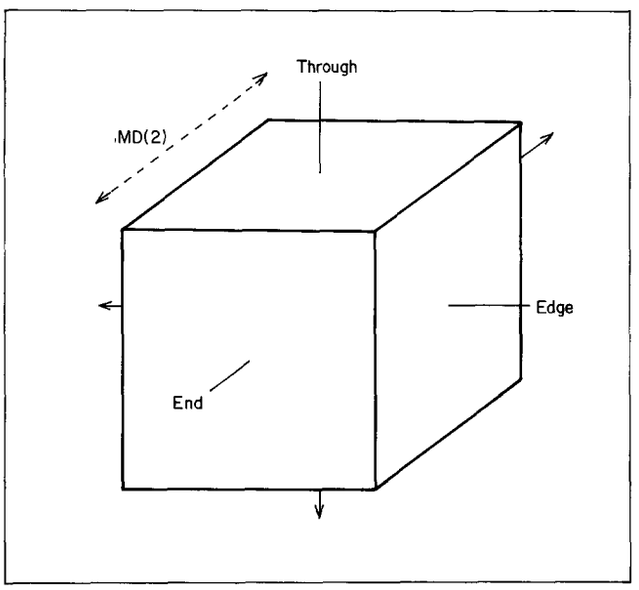

Figure 1 Schematic diagram of specimen setting for X-ray diffraction: MD(2): the second stretching direction

RESULTS AND DISCUSSION

Figure 2 shows the wide-angle X-ray diffraction patterns of a film obtained by two-step transverse stretching (70°C–90°C). The end view pattern indicates a very sharp 6-point diagram. This indicates that the *b*-axis orients sharply within the cross-section perpendicular to the stretching direction (the end plane).

In general, there are two possible double orientations in the 6-point diagram, for a crystal with a hexagonal structure as shown in *Figure 3a-1* and *3a-2*. The *b*-axis orients at 90° ($\phi_b = 90°$) and at 30° ($\phi_b = 30°$) to the normal direction of the film surface. The *β*-crystal of PVDF has a pseudohexagonal structure[12] and therefore it could be theoretically possible to distinguish the (200) reflection from the (110) reflection. However, no separation of the (200) and (110) reflections was observed at each point of the 6-point diagram in the 'end' view photograph.

In addition, the structure factors of the *β*-crystal calculated by Takahashi *et al.*[13] are 1.68 and 1.0 for $F|(110)|^2$ and $F|(200)|^2$ respectively, thus making it impossible to determine whether a reflection belongs to either the (110) or the (200) reflections. Therefore, we cannot distinguish the two different double orientations from one another. However, fortunately among other reflections composed of several independent reflections (*hkl*) with nearly the same Bragg angle, the structure factors of $F|(201)|^2$ and $F|(111)|^2$ are calculated to be 0.00 and 1.00 respectively. Therefore, the observation of the reflection will be perfectly suitable for determining the *b*-axis orientation. The structure factors $F|(021)|^2$ and $F|(311)|^2$ are 5.61 and 1.00 respectively, so we can also assume a combination of the (021) and (311) reflections or the (021) reflection.

The rotating axis for the rotation photographs was selected to be normal to the film surface, and thus the (111) and (021) reflections will appear as shown in *Figure 3b-1* and *3b-2* for the two types of double orientations ($\phi_b = 90°$ and 30°). In the case of the $\phi_b = 90°$ orientation, the (111) reflection will appear only on the first layer line and the (021) reflection will appear on the equatorial line. In the

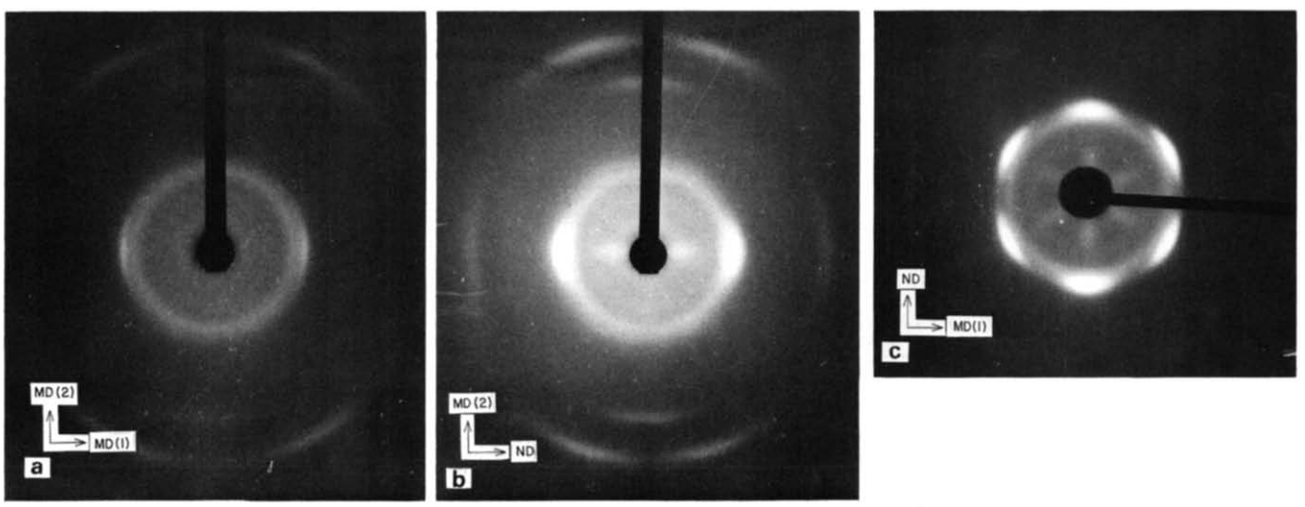

Figure 2 X-ray diffraction photographs of the two-step transversely stretched film (70°C–90°C), taken with a flat camera (40 mm, CuKα) in the direction of 'through' (a), 'edge' (b) and 'end' (c) respectively. MD(1): the first stretching direction; MD(2): the second stretching direction; ND: the direction normal to the film surface

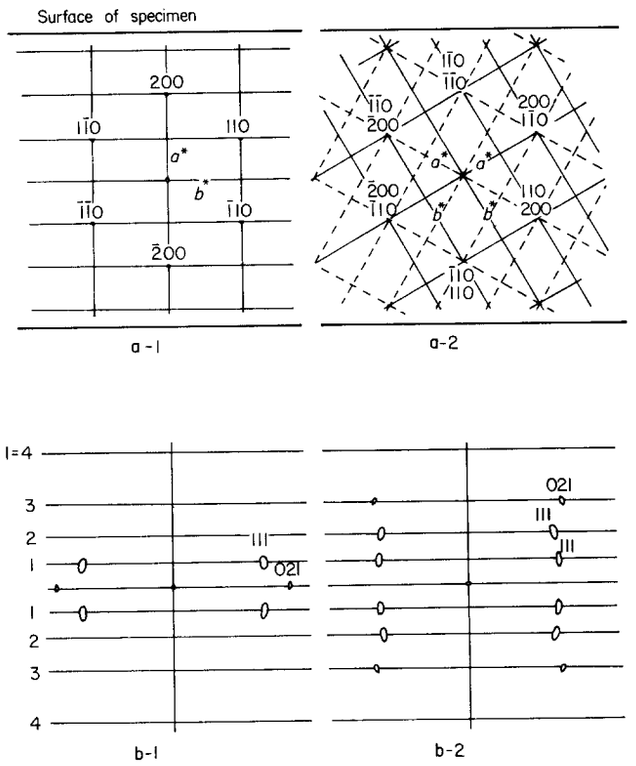

Figure 3 Two types of possible double orientation in 6-point diagram: (a) space arrangements of reciprocal lattices in specimen; (b) schematic representations of cylindrical camera photographs, where only (111) and (021) reflections are shown with proportionality to their observed intensities. 1: $0_b = 90°$ orientation; 2: $0_b = 30°$ orientation

case of $\phi_b = 30°$ orientation, the (111) reflection will appear on the first and second layer lines and the (021) reflection on the third line. In the case of $\phi_b = 90°$ and 30° orientations, the (111) reflection will naturally appear on the first and second layer lines, and also the (021) reflection on the equatorial and third layer lines.

The cylindrical camera photograph taken for the two-step transversely stretched film (70°C–90°C) is shown in *Figure 4a*. Since the (111) reflection appears only on the first layer line and the (021) reflection only on the equator, we can conclude that this film has the double orientation of $\phi_b = 90°$. On the other hand, in the photograph for the two-step transversely stretched film (70°C–155°C) shown in *Figure 4b*, the (111) reflection appears in the first and second layer lines, and the (021) reflection in the equator and the third layer lines. Therefore, we can conclude that this film has the mixed double orientations of $\phi_b = 90°$ and 30°.

We have observed that the $\phi_b = 90°$ orientation is obtained when both the first and second stretching temperatures are below 100°C. The level of double orientation was improved as the quenching, first and second stretching temperatures were lowered. The best $\phi_b = 90°$ orientation was obtained when the original sheet was obtained by quenching in dry-ice–methanol (−80°C) and stretched at (25°C–125°C). When the second stretching temperature was above 100°C, we could observe both $\phi_b = 90°$ and 30° orientations and the proportion of the latter was increased when the stretching temperature was raised.

In order to clarify the effect of heat-treatment, a $\phi_b = 90°$ oriented film obtained by stretching at (70°C–90°C) was heat-treated at 140°C for 4.5 h. The 'end' view X-ray photograph retained a typical 6-point diagram, but the (111) reflection can be seen on the first and second layer lines and the (021) reflection on the equator and third layer lines for the cylindrical camera photograph. It is apparent that the $\phi_b = 90°$ orientation was partially rotated through 60° by the heat-treatment process.

The reasons why these crystal orientations are obtained can be understood on the basis of the data contained in the measurements of the crystal spacings.

In order to observe as many diffraction spots as possible and hence calculate the spacings of crystal planes, a set of oscillation photographs were taken for each sample with the incident X-ray beam angles set for every 10 degrees between the 'end' view and the 'edge' view. The rotating axis of the specimen was set perpendicular to the film surface and the rotating angle is within ±15°.

Figure 5 shows the lattice spacings of the *a*-, *b*- and *c*-axis for the two-step transversely stretched films which were first stretched at 70°C and secondly stretched at

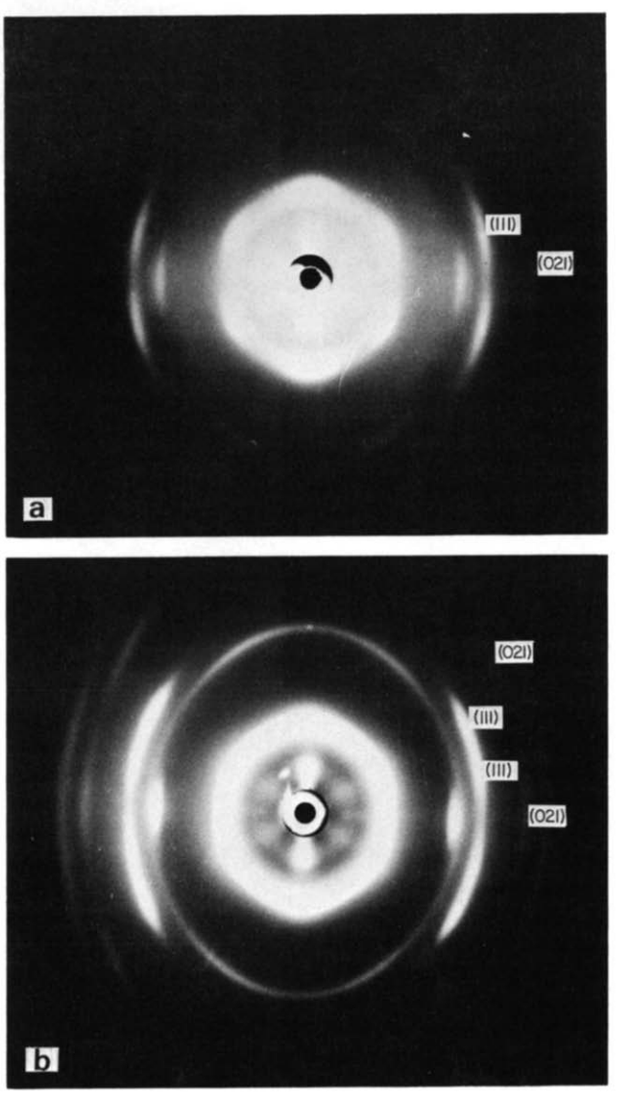

Figure 4 Rotation photographs of the two-step transversely stretched films taken with a cylindrical camera (35 mm, CuKα): (a) (70°C–90°C); (b) (70°C–155°C)

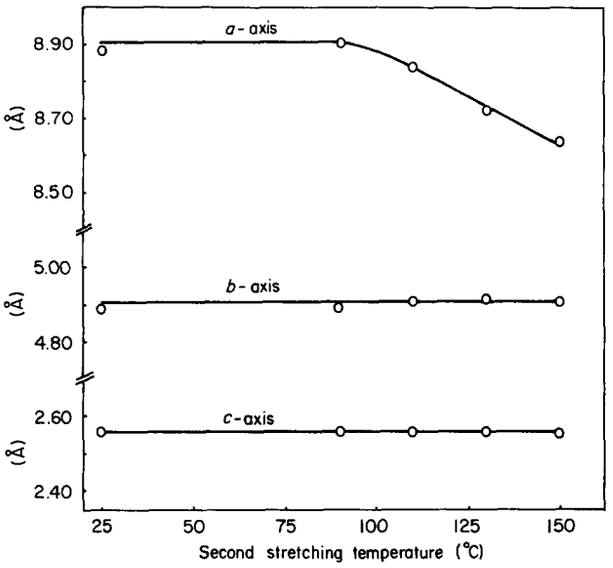

Figure 5 Relationship of the lattice constants to the second stretching temperature for films first uniaxially stretched at 70°C

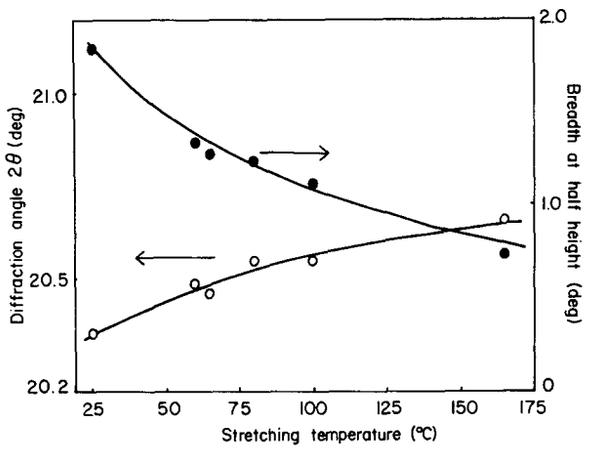

Figure 6 Relation of peak position and breadth at half height of the (200)+(110) reflection to the stretching temperature for uniaxially stretched films

various temperatures between 25°C and 155°C. In *Figure 5* the abscissa indicates the lattice spacings of the *a*-, *b*- and *c*-axes. As shown in *Figure 5*, the lattice spacings of the *a*-axis of the double orientation films stretched below 110°C is considerably expanded (about 8.90 Å). On the other hand, as the stretching temperature is raised (above 110°C), the *a*-axis is reduced. The *a*-axis of the film for T_1–T_2=70°C–155°C is 8.61 Å. This value is still slightly larger than the normally accepted value; 8.58 Å[11]. Furthermore, J. B. Lando *et al.*[14] and YE. L. Gal'perin *et al.*[15] have reported 8.47 Å and 8.45 Å, respectively. The lattice spacings of the *b*-axis and *c*-axis of these films do not depend on the stretching temperatures and are in good agreement with Hasegawa's data; b=4.91 Å and c=2.56 Å[11]. Therefore, *Figure 5* shows that the lattice spacing of the *a*-axis is increased when the stretching temperatures are below 100°C. This would indicate that the lattice in the *a*-axis direction is loosely packed during the stretching process. When the stretching temperature is above 100°C, this loosely packed structure may be heat-treated and it relaxes with the lattice spacing reducing to a value close to that shown in the hexagonal structure.

The apparent plane spacings of the (200)+(110) reflection are given for the uniaxially stretched films at various temperatures in *Figure 6*. These apparent reflection angles and breadths at half height were obtained by reading the centre position and the breadth at half height of the reflection peak, which shows a single peak although the peak is a combination of (200) and (110) reflections. When the stretching temperature is lowered, the (200) and (110) reflection spacing becomes larger and the half width of the peak becomes larger. These results probably indicate that the spacing of the (200) plane is also increased for the first uniaxial stretching at low temperature.

When the uniaxially stretched film is stretched again, perpendicular to the first stretching direction, the direction of the chain axis (*c*-axis) is compelled to turn at right angles within the plane of the film, so that a large shearing stress parallel to the film surface is applied to the crystals. That is, the cross-section perpendicular to the chain axis which contains the *a*- and *b*-axes is compelled to deform by this large shearing stress. The (200) plane having the largest spacing and parallel to the zig-zag plane of the all-*trans* molecular chain must orient parallel to the film surface. As shown in *Figures 5* and *6*, the spacings of the *a*-axes of these films were decreased for stretching temperatures above 100°C, this means that these stretching temperatures also act, as the heat-treatment effect, and the heat-treatment relaxes the expanded plane spacings to close to the normal value. In this case, the contribution of the (200) to the deformation as the slip plane will decrease and the deformation will start so as to slip along the (110) slip plane, because the (110) can work well as a slip plane in a hexagonal crystal structure.

It was claimed by Wang[10] on the basis of a 6-point diagram obtained from as 'end' view photograph that a $\phi_b=0°$ oriented film with a 'single crystal orientation' was obtained. However, as explained before, it is nearly impossible using only the 6-point diagram to distinguish between the two different double orientations. We tried to produce the same type of the film with Wang's procedure; first uniaxially stretching and then rolling. The 'end' view photograph of the two-step stretched and rolled film shows the same pattern as indicated by Wang (*Figure 7*); that is, a pair of reflection spots in the 6-point diagram exist in the direction parallel to the film surface. This pattern is different from the 'end' view photographs of the two-step transversely stretched films, where a pair of reflection spots exist in the direction normal to the film surface (see *Figure 2c*). To examine these samples, the rotating axis in the measurements by the cylindrical camera should be parallel to the direction of a pair of reflection spots. Therefore, the two-step stretched and rolled films were set in the cylindrical camera, where the normal axis to the 'edge' plane of the film is adopted as the rotating axis, which contains a pair of reflection spots as shown in *Figure 7*.

Figures 8a and *8b* are the cylindrical camera photographs for the films which were produced by stretching at 70°C and 165°C and then rolled at room temperature. *Figure 8c* shows the films stretched at 165°C, and rolled at room temperature and annealed at 150°C for 4.5 h. In *Figure 8a*, the (111) reflection spots appear in both the first and second layer lines and the (021) reflection spots appear only in the third layer line. Therefore, we conclude that the *b*-axis is oriented at 30° to the film surface; that is, this film has the $\phi_b=60°$ orientation.

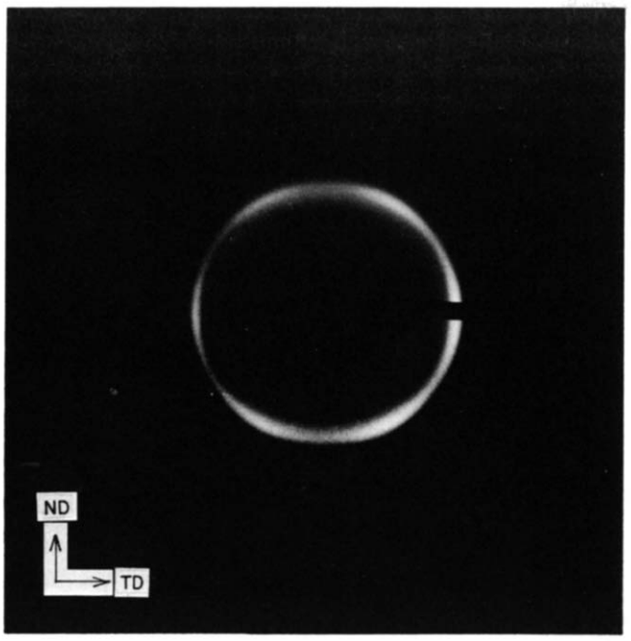

Figure 7 'End' view X-ray diffraction photograph of two-step stretched and rolled film, taken with a flat camera (40 mm, CuKα). TD: the transverse direction to the stretching and rolling direction. ND: the direction normal to the specimen film surface

On the other hand, in *Figures 8b* and *8c*, the (111) reflection spots appear in both the first and second layer lines, and the (021) reflection spots appear in both the equator and the third layer lines; therefore, we conclude that these films have mixed orientations of $\phi_b = 60°$ and 0°. The lattice spacings of these two-step stretched and rolled films were measured and calculated with the help of mainly (001), (002), (310) and (021) reflections. These results were plotted in *Figure 9*, where the abscissa indicates the first stretching temperature (T_3) and the ordinate indicates the lattice spacings of the *a*-, *b*- and *c*-axes. These uniaxially stretched specimens were then rolled at room temperature. *Figure 9* shows that the spacings of the *a*-axis of these films were nearly constant, about 8.64 Å for T_3 from 60°C to 165°C. That is, the spacings of the *a*-axis of these films are not dependent on the stretching temperature (T_3), and seem to be dependent on the rolling temperature (T_R). However, in the range for T_3 from 60°C to 165°C, the two kind of orientations exist; $\phi_b = 60°$ and $\phi_b = 60° + 0°$. A thin section of the film shown in *Figure 8b* was cut at right angles to the stretching and rolling direction and transmission micrographs of the specimen were taken. Numerous lines are observed, inclined on both sides at about 60°C to the normal axis. This indicates that the film was deformed along these lines by compression during rolling.

We recognized that the degree of the *c*-axis orientation did not change during rolling at room temperature, indicating that the polymer chains are fully extended in the uniaxially stretched film. Therefore, when the uniaxially stretched film is compressed, the deformation will take place within the (*hk*0) planes. There are two possibilities of deformation such as a slipping mechanism and a twinning mechanism. Since the spacing of the (200) plane possesses the largest spacing, it seems natural that the (200) plane acts as a slip plane or a twin plane. Hence, the largest shear stress will affect the crystals which have the (200) planes oriented about 45° to the film surface, resulting in the orientation of the (200) plane at about 60° to the film surface.

The films uniaxially stretched above 100°C gave a mixture of $\phi_b = 60°$ and 0° orientations after rolling at room temperature, judging from the fact that the (021)

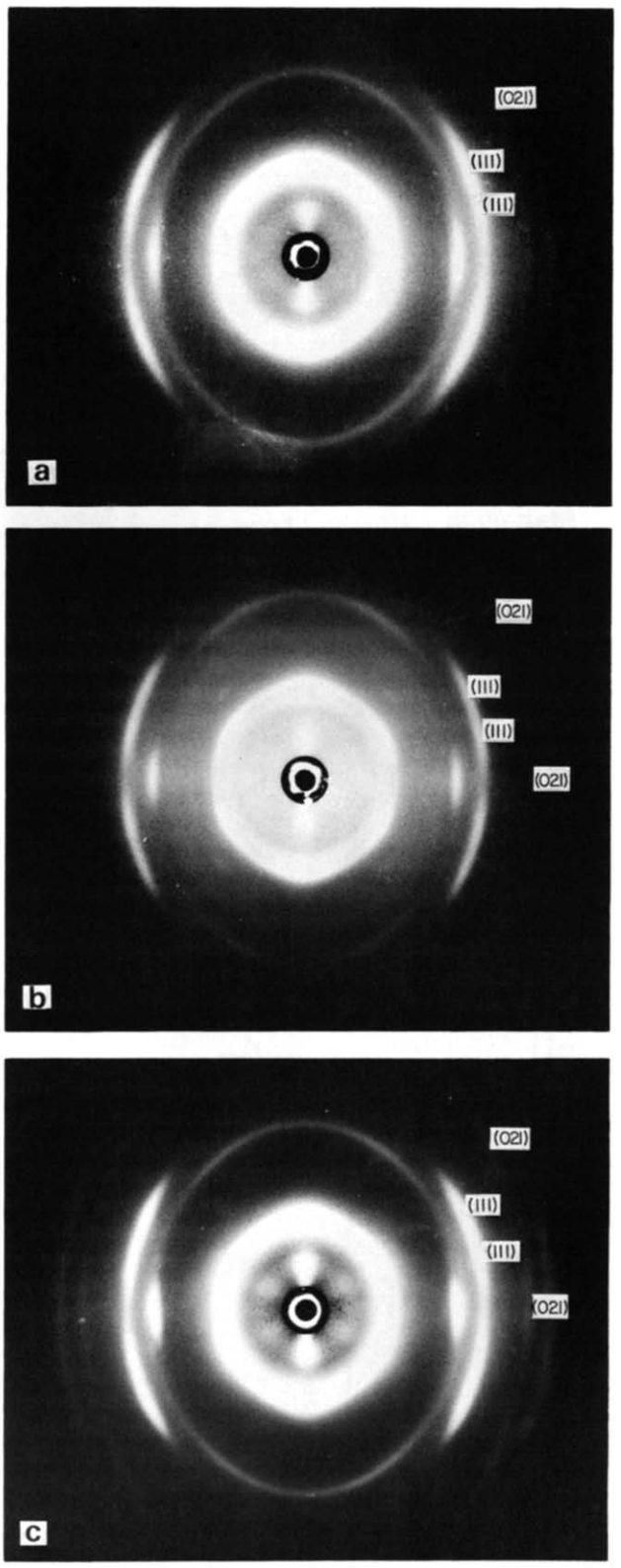

Figure 8 Rotation photographs of two-step stretched and rolled films, taken with a cylindrical camera (35 mm, CuKα). (a) stretched at 70°C and then rolled without annealing; (b) stretched at 165°C and then rolled without annealing; (c) stretched at 165°C, then rolled and annealed at 150°C for 4 h

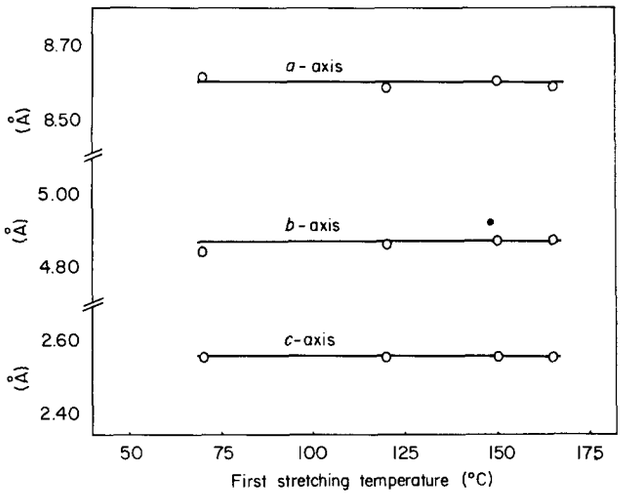

Figure 9 Relationship between the first stretching temperature (T_3) and the lattice constants (*a*, *b* and *c*-axes)

reflection also appears on the equator. This is probably because both (200) and (110) planes can be involved in deformation as a result of the more perfect hexagonal structure. If the $\phi_b = 60°$ oriented film was heat-treated at temperatures above 100°C (preferably 140°C), the $\phi_b = 60°$ and 0° orientations were observed. The heat-treatment brings about the 60° rotation of the *b*-axis. Wang proposed at first a crystal orientation of $\phi_b = 0°$ for the film obtained by stretching uniaxially, rolling and annealing. Recently he corrected his first model and gave $\phi_b = 60°$ orientation[16]. However, we obtained the $\phi_b = 60°$ oriented film as well as the $\phi_b = 60° + 0°$ oriented film. The contradiction can be understood from the fact that any structural analysis on the basis of the (200) and (110) reflections or any other (*hkl*) reflections will not be conclusive, because the different reflections have nearly the same Bragg angles and comparable structural factor values.

CONCLUSIONS

(1) By uniaxially stretching below 100°C a PVDF film quenched from the melt and then by stretching the same film at below 100°C in the direction perpendicular to the first stretching direction ('two-step transversely stretching'), a doubly oriented film is obtained, in which the *c*-axis and *b*-axis are oriented parallel to the stretching direction and parallel to the film plane respectively ($\phi_b = 90°$ orientation). When either the first or second stretching temperature is above 100°C, the resultant film contains both $\phi_b = 90°$ and 30° orientations.

(2) By uniaxially stretching the sheet obtained from the melt below 100°C and rolling the consequent film at room temperature ('two-step stretching and rolling'), a doubly oriented film is obtained, in which the *c*-axis and *b*-axis are oriented parallel to the stretching direction and at an angle of 60° to the direction normal to the film plane ($\phi_b = 60°$ orientation). When the first stretching temperature is above 100°C, the resultant film contains both $\phi_b = 60°$ and 0° orientations.

(3) The heat-treatment of both 90°-oriented and 60°-oriented films at rather high temperatures usually generates the 30° and 0° orientations, respectively. We have shown that the 60°-rotation of *b*-axis is due to the heat-treatment.

(4) By analysing the diffraction pattern for the $\phi_b = 90°$ oriented film, an expansion of the spacing of the (200) plane is observed. It is speculated that the expanded (200) plane might take part in the deformation of the two-step transversely stretching as a slip plane and in the deformation of the two-step stretching and rolling as a slip plane or twin formation.

REFERENCES

1 Kawai, H., *Jpn. J. Appl. Phys.* 1969, **8**, 975
2 Gal'perin, Ye. L. *et al. Vysokomol. Soyed.* 1965, **7**, 933
3 Okuda, K. *et al. Polym. Lett.* 1967, **5**, 465
4 Doll, W. W. and Lando, J. B. *J. Macromol. Sci. Phys.* 1968, **B2**, 219
5 Weinhold, S. *et al. J. Polym. Sci. Polym. Lett. Edn.* 1979, **17**, 585
6 Das-Gupta, D. K. and Doughty, K. *J. Appl. Phys.* 1978, **49**, 4601
7 Davies, G. R. and Singh, H. *Polymer* 1979, **20**, 772
8 Murayama, N. *et al. J. Polym. Sci. Polym. Phys. Edn.* 1975, **13**, 1033
9 Bunn, C. W. 'Chemical Crystallography' (Second Edition), Oxford (1961), p. 191
10 Wang, T. T. *J. Appl. Phys.* 1979, **50**, 6019
11 Hasegawa, R. *et al. Polym. J.* 1972, **3**, 600
12 Kepler, R. G. and Anderson, R. A. *J. Appl. Phys.* 1978, **49**, 1232
13 Takahashi, N. and Odajima, A. Extended Abstracts, The International Workshop and Electric Charges in Dielectrics, Kyoto, (1978), p. 88
14 Lando, J. B. *et al. J. Polym. Sci. A-1* 1966, **4**, 941
15 Gal'perin, Ye. L. *et al. Vysokomol. Soyed.* 1965, **7**, 933
16 Brasen, D. and Wang, T. T. *J. Appl. Phys.* 1981, **52**, 5543